Post-fabrication frequency trimming of coplanar-waveguide resonators in circuit QED quantum processors

Vallés-Sanclemente, S.; van der Meer, S. L.M.; Finkel, M.; Muthusubramanian, N.; Beekman, M.; Ali, H.; Marques, J. F.; Zachariadis, C.; Veen, H. M.; Stavenga, T.

Citation (APA)
Vallés-Sanclemente, S., van der Meer, S. L. M., Finkel, M., Muthusubramanian, N., Beekman, M., Ali, H., Marques, J. F., Zachariadis, C., Veen, H. M., Stavenga, T., Haider, N., & DiCarlo, L. (2023). Post-fabrication frequency trimming of coplanar-waveguide resonators in circuit QED quantum processors. *Applied Physics Letters*, *123*(3), Article 034004. https://doi.org/10.1063/5.0148222

Important note
To cite this publication, please use the final published version (if applicable).
Please check the document version above.

Post-fabrication frequency trimming of coplanar-waveguide resonators in circuit QED quantum processors

S. Vallés-Sanclemente ; S. L. M. van der Meer ; M. Finkel ; N. Muthusubramanian ; M. Beekman ;
H. Ali ; J. F. Marques ; C. Zachariadis ; H. M. Veen ; T. Stavenga ; N. Haider ; L. DiCarlo ✉

Check for updates

View Online

Export Citation

CrossMark

AIP
Publishing

Post-fabrication frequency trimming of coplanar-waveguide resonators in circuit QED quantum processors ⓕ

View Online   Export Citation   CrossMark

S. Vallés-Sanclemente,[1,2] ⓘ S. L. M. van der Meer,[1,2] ⓘ M. Finkel,[1,2] ⓘ N. Muthusubramanian,[1,2,a] ⓘ
M. Beekman,[1,3] ⓘ H. Ali,[1,2] ⓘ J. F. Marques,[1,2] ⓘ C. Zachariadis,[1,2,b] ⓘ H. M. Veen,[1,2] ⓘ T. Stavenga,[1,2]
N. Haider,[1,3] ⓘ and L. DiCarlo[1,2,c] ⓘ

AFFILIATIONS

[1]QuTech, Delft University of Technology, P.O. Box 5046, 2600 GA Delft, The Netherlands
[2]Kavli Institute of Nanoscience, Delft University of Technology, P.O. Box 5046, 2600 GA Delft, The Netherlands
[3]Netherlands Organisation for Applied Scientific Research (TNO), P.O. Box 96864, 2509 JG The Hague, The Netherlands

[a]Present address: QphoX B.V., Elektronicaweg 10, 2628 XG Delft, The Netherlands.
[b]Present address: Quantware B.V., Elektronicaweg 10, 2628 XG Delft, The Netherlands.
[c]Author to whom correspondence should be addressed: l.dicarlo@tudelft.nl

ABSTRACT

We present the use of a set of airbridges to trim the frequency of microwave coplanar-waveguide (CPW) resonators post-fabrication. This method is compatible with the fabrication steps of conventional CPW airbridges and crossovers and increases device yield by allowing compensation of design and fabrication uncertainty with 100 MHz range and 10 MHz resolution. We showcase two applications in circuit QED. The first is the elimination of frequency collisions between resonators intended to readout different transmons by frequency-division multiplexing. The second is frequency matching of readout and Purcell-filter resonator pairs. Combining this matching with transmon frequency trimming by laser annealing reliably achieves fast and high-fidelity readout across 17-transmon quantum processors.

Accurate targeting of qubit and resonator frequencies is increasingly important as quantum information processors scale. Deviations from targeted resonance frequencies, arising from design limitations and fabrication uncertainly, will, otherwise, bottleneck the yield of fully operable devices.[1] Poor targeting of qubit frequencies is a primary cause of crosstalk induced by microwave-frequency drives[2] and can limit gate speed.[3–5] It also increases residual ZZ coupling in processors with always-on qubit–qubit coupling,[2,6,7] making gate fidelity and leakage dependent on the state of spectator qubits.[8] For these reasons, qubit frequency targeting has received particular focus in recent years, with laser annealing of constituent Josephson junctions becoming the established post-fabrication trimming method.[1,9–11] Laser annealing allows selective and controlled reduction of transmon qubit frequencies over a few hundred MHz without intrinsic impact on coherence times.

Comparatively, post-fabrication trimming of resonators has received less focus to date. Generally, CPW resonators for readout and qubit–qubit coupling do not use Josephson junctions, and their frequencies are mainly set by geometry.[12,13] However, unaccounted

capacitive loadings and variations in CPW phase velocity ν_ρ can affect the frequency separation of resonators meant to readout different qubits by frequency-division multiplexing with a common feedline.[14] They also prevent achieving the resonance of readout resonators with their individual Purcell-filter resonators, used in a recent approach[15] to break the traditional trade-off between readout speed and qubit relaxation through the Purcell effect.[16] One path to alleviate these problems is making resonators flux tunable.[17] However, it requires extra on-chip elements such as Josephson-junction loops and dedicated flux-control lines and can limit the dynamic range.

In this Letter, we introduce a simple airbridge-based method, nicknamed *shoelacing*, enabling frequency trimming of microwave CPW resonators after fabrication and initial characterization. In the circuit QED context, we show that the 100 MHz trimming range with 10 MHz resolution allows correcting frequency mistargeting due to chip design and fabrication uncertainty in 17-transmon quantum information processors[18] (named Surface-17). The origin of this uncertainty in our devices is primarily the within-wafer and wafer-to-wafer

variation of the thickness of the NbTiN base layer, which affects the kinetic-inductance contribution to ν_ρ.[19] First, we fix frequency collisions of the resonators used for dispersive readout of different transmons using a common feedline. Next, we demonstrate the frequency matching of dedicated readout and Purcell-filter resonator pairs. Used in combination with transmon trimming by laser annealing, we achieve fast (400 ns) and high-fidelity (98.6% average) readout on all transmons that are not limited by known extraneous factors. A key advantage of shoelacing is the simultaneous fabrication with conventional CPW airbridges and crossovers, avoiding extra device processing during fabrication.

Individual qubit readout in Surface-17 is based on the quantum-hardware architecture set forth by Heinsoo et al.,[15] illustrated in Fig. 1(a). A transmon (T), with qubit transition frequency f_T, couples with strength g to a dedicated $\lambda/4$ readout resonator (R) with frequency f_R. In the dispersive regime, where $\Delta_{RT} = 2\pi \times (f_R - f_T) \gg g$, exciting T from its ground to first-excited state ($|0\rangle$ and $|1\rangle$, respectively) introduces a shift 2χ in the frequency of R. R also couples with strength J to a dedicated $\lambda/4$ Purcell-filter resonator (P) at f_P. Finally, P couples with rate κ to a 50 Ω feedline whose output connects to an amplification chain with a traveling-wave parametric amplifier (TWPA)[20] at its front end, which provides ~20 dB gain in the readout frequency band (7–8 GHz). Target design values for the coupling rates and Δ_{RT} are summarized in Table I. Ideally, $\Delta_{PR}/2\pi = f_P - f_R = 0$, so that R and P fully hybridize into two readout modes that frequency-split by $2J$, each with effective linewidth $\kappa_{eff} = \kappa/2$ and dispersive shift $2\chi_{eff} = \chi$. High κ_{eff} is necessary for fast readout as it sets the rate at which the readout mode builds/depletes internal photon population when the pulse is turned on/off. Independent readout of multiple transmons using a common feedline is possible by frequency-division multiplexing, provided that the hybridized modes for different transmons do not overlap in frequency. For each transmon, a readout pulse of duration τ_p is applied to the feedline input, at a frequency f, where transmission is dependent on qubit state.

The aforementioned description sets the stage for understanding the complications arising when R and P resonators are not well targeted due to chip design error and/or fabrication variability. The example in the top panel of Fig. 1(b) shows two key problems. First, there is a striking difference in the linewidths of the two modes for each resonator pair, indicating that R and P are detuned. These linewidths are given by,[15]

$$\kappa_{eff} = \frac{1}{2}\left(\kappa \pm \mathrm{Re}\left\{\sqrt{-16J^2 + (\kappa - 2i\Delta_{PR})^2}\right\}\right), \quad (1)$$

with negative sign for the mode that has a larger contribution from R than P. Second, there is a frequency collision between modes for two different transmons, as highlighted by the shaded red region.

To solve these problems, we place 10 superconducting airbridges (2 μm width and 5 μm pitch), which ground the short-circuited end of each R and P CPW resonator [Fig. 1(c)]. Each shoelace contacts the CPW center conductor to the flanking ground planes on both sides, shortening the resonator while preserving the symmetry of the termination. The removal of the n shoelaces farthest away from the short-circuit on the base layer increases the resonator length by $\Delta l = n \times 5$ μm and decreases its frequency by
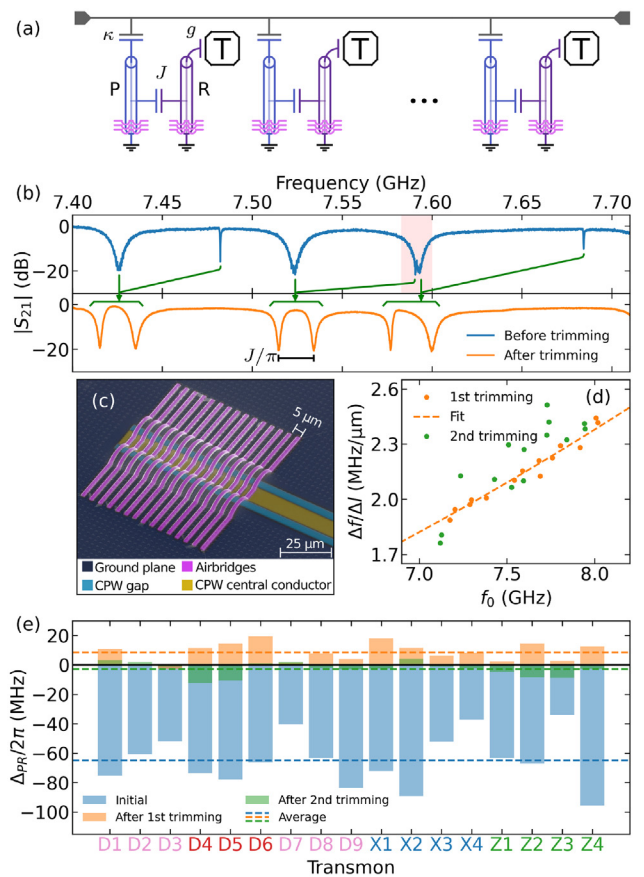
FIG. 1. (a) Schematic of the architecture[15] used to readout multiple transmons (T) using frequency-division multiplexing on a common feedline. Each transmon has a dedicated readout (R) and Purcell-filter (P) resonator (see the text for details). (b) Top panel: Initial characterization of feedline transmission in the frequency range of three readout-Purcell resonator pairs. The pairs are detuned, as evidenced by the difference in linewidth of their hybridized modes. The red region shows the crowding of readout modes for different transmons. Bottom panel: Characterization of feedline transmission after one trimming cycle. The matching of R and P resonators is significantly improved, and the frequency collision resolved. (c) False-colored scanning-electron micrograph of the shoelaces placed near the short-circuit end of a $\lambda/4$ CPW resonator. (d) Change in resonator frequency normalized to the change in length as a function of the pre-trimming frequency. Data are shown for two trimming cycles. The best fit of Eq. (2) to the data from the first-cycle gives $\nu_\rho = 1.076 \times 10^8$ m/s. (e) Detuning $\Delta_{PR}/2\pi$ between the R and P resonators for all transmons in the Surface-17 processor, measured post-fabrication (blue) and after each of the trimming cycles (orange and green). The dashed lines indicate the average for each characterization. The naming of transmons follows the surface-code convention detailed in Ref. 18.

$$\Delta f \approx -\frac{4f_0^2}{\nu_\rho}\Delta l, \quad (2)$$

where f_0 is the resonator frequency during characterization. The geometry, number, and pitch of shoelaces are chosen to enable a 100 MHz trimming range with 10 MHz resolution, and low chance of human error when plucking shoelaces using a fine needle under an optical microscope. While removal allows only a monotonic decrease

TABLE I. Target values for the coupling rates in the qubit-resonator-Purcell system and for the qubit-resonator frequency detuning.

Parameter	Symbol	Target value
Coupling strength between the Purcell filter and feedline	$\kappa/2\pi$	20 MHz
Coupling strength between the Purcell filter and readout resonator	$J/2\pi$	10 MHz
Coupling strength between the readout resonator and qubit	$g/2\pi$	200 MHz
Frequency detuning between the readout resonator and the qubit	$\Delta_{RT}/2\pi$	1–2.3 GHz

in resonator frequency, having shoelaces on both R and P resonators allows bidirectional trimming of Δ_{PR}.

To determine the required trimming Δf for a resonator, an initial characterization is conducted with all transmons biased at their sweet-spot. Except for cases with evident frequency collisions, f_R and f_P can be determined by fitting a feedline transmission (S_{21}) measurement to Ref. 15,

$$S_{21}(f) = 1 - \frac{2i\kappa\Delta_R}{4J^2 + (2i\Delta_P + \kappa)2i\Delta_R},\tag{3}$$

where $\Delta_{P,R}/2\pi = f_{P,R} - f$. Here, f_R includes the Lamb shift induced by transmon coupling.[21] We remove the contribution from the Lamb shift by numerically solving the Hamiltonian for a resonator coupled to a transmon that is modeled as a Duffing oscillator, extracting the bare resonator and transmon transition frequencies.[22]

One cycle of shoelace plucking solves both the frequency collision and the large detuning of R and P resonators for each transmon, as shown by the bottom panel of Fig. 1(b). An overshoot in Δf is generally observed for this cycle [Fig. 1(e)]. This is most likely due to naively approximating Eq. (2) as $\Delta f \approx a\Delta l$ with $a = -2$ MHz/μm. To correct this, we perform a second trimming cycle using Eq. (2) with $\nu_\rho = 1.076 \times 10^8$ m/s extracted from best fits of this equation to first-cycle data. Evidently, the second cycle brings Δ_{PR} even closer to target.

Matching R and P resonators for high κ_{eff} is one of two key ingredients for fast and high-fidelity dispersive readout. The second is satisfying $|2\chi_{eff}| \lesssim \kappa_{eff}$ to maximize the signal-to-noise ratio at fixed photon number in the readout mode.[23,24] Transmon frequency trimming by laser annealing can be relied on to achieve this condition because f_T affects 2χ. In the example of Fig. 2(a), a low and positive Δ_{RT} caused by a mistargeted high f_T makes $|2\chi|$ too large. There is also a strong R and P mismatch. In combination, these effects make $|2\chi_{eff}/\kappa_{eff}| \approx 20$ for the lower-frequency mode and ~ 0.01 for the higher-frequency mode. To fix this, we make use of both shoelacing and laser annealing in the same trimming cycle to decrease f_P and f_T, respectively. The improved matching and decreased 2χ give $|2\chi_{eff}/\kappa_{eff}| \approx 0.7$ (0.4) for the lower (upper) hybridized mode. Using the mode, the photon depletion time for a fixed readout pulse amplitude decreases from >1 μs before trimming to 280 ns after trimming, as evaluated with an experiment based on Ref. 25 [Fig. 2(c)]. Optimizing the readout pulse amplitude, f and τ_p using the procedures presented in the supplementary material reach readout fidelity $F_{RO} = 98.9\%$ with a total readout time $\tau_{RO} = 400$ ns (including τ_p
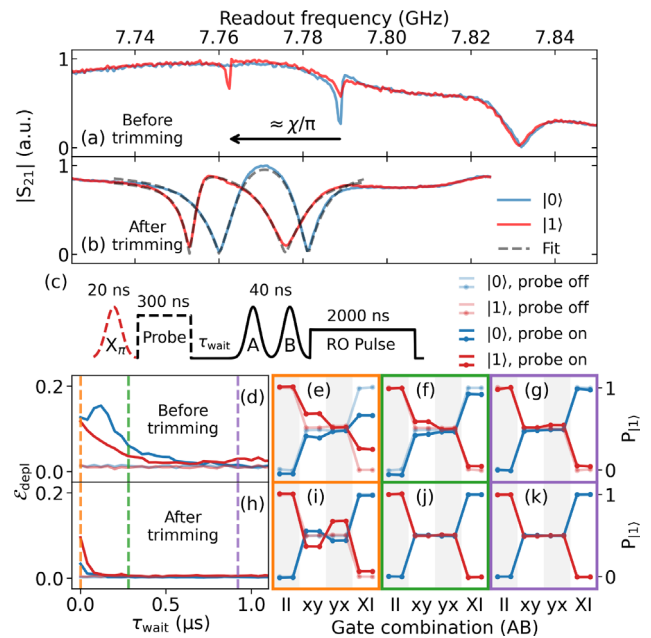

FIG. 2. (a) Feedline transmission in the frequency range of the readout-Purcell resonators of transmon D_4, when prepared in $|0\rangle$ (blue) and $|1\rangle$ (red). (b) Similar feedline transmission after resonator and qubit frequency trimming. (c) Experiment used to determine the photon depletion time. A probe readout pulse with a fixed duration and amplitude is followed by two back-to-back single-qubit gates AB $\in \{II, xy, yx, XI\}$ and a calibrated readout pulse. (d) Deviation from ideal performance of gates AB before trimming. The probe pulse frequency is set to 7.789 GHz (7.762 GHz) for preparation in $|0\rangle$ ($|1\rangle$). The light blue and red traces were acquired without the probe pulse and are displayed for reference. (e)–(g) Raw measurement outcomes for $\tau_{wait} = 0$, 0.28, and 0.92 μs for the dataset acquired before trimming. (h) Deviation from ideal performance of gates AB, after trimming. The probe pulse frequency is set to 7.760 GHz (7.753 GHz) for preparation in $|0\rangle$ ($|1\rangle$). (i)–(k) Raw measurement outcomes at the same τ_{wait} settings as in panels (e)-(g).

and photon depletion time) and keeping the readout highly non-demolition.[7] These results conclusively show the benefits of combining resonator and transmon trimming to accelerate and improve qubit readout.

To demonstrate the reliability of combining these trimming methodologies, we entrust them to optimize readout on the actual Surface-17 that we use for QEC experiments. In total, we trimmed 16 of the 34 resonators (either R or P for each case) and 11 of the 17 transmons. Transmon trimming for optimized readout was sufficiently mild to keep residual ZZ coupling low. Figure 3(b) displays the readout assignment error $\varepsilon_{RO} = 1 - F_{RO}$ achieved for all transmons, with common $\tau_{RO} = 400$ ns and individually optimized τ_p. The high errors observed in transmons X_2 and X_4 are due to extraneous sources: X_2 is coupled to a two-level system at its sweetspot (the bias point), and feedline transmission at the readout frequency of X_4 shows a strong anomalous ripple, attributed to the TWPA. Excluding these, the average ϵ_{RO} is 1.45%.

In summary, we have introduced and realized shoelacing, a post-fabrication trimming method for CPW resonators. The results showcase the effectiveness of the method in a circuit QED context, solving frequency collisions in readout feedlines and improving the frequency matching of readout and Purcell-filter resonator pairs. Combining
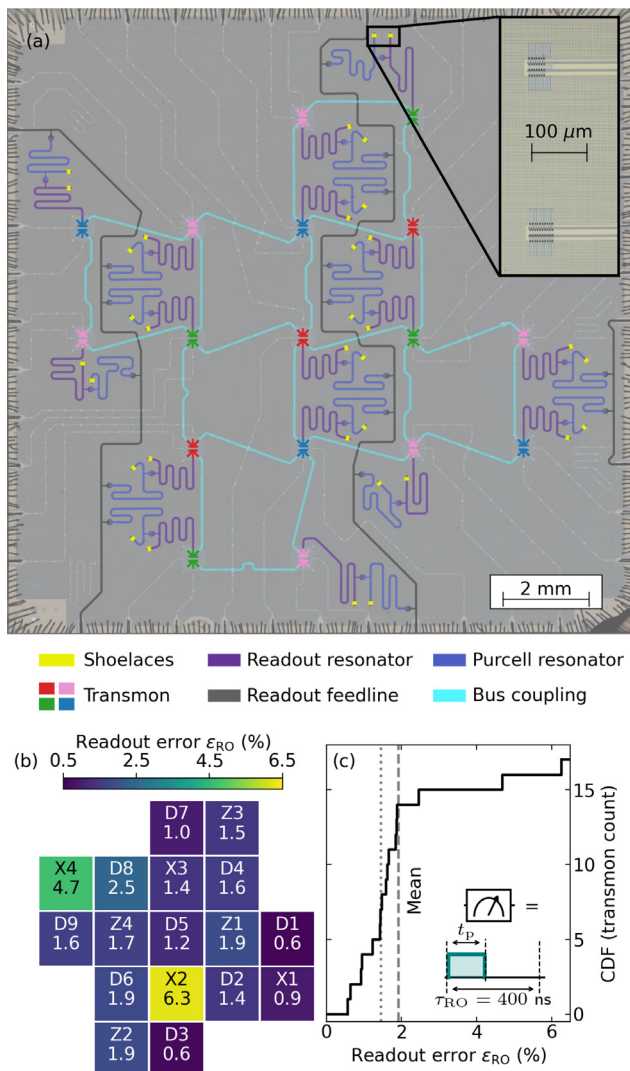
FIG. 3. (a) Optical image of our Surface-17 processor used for the distance-3 surface code.[18] All transmons have dedicated readout and Purcell resonator pairs with shoelaces enabling their frequency trimming. Inset: Close-up showing the short-circuit ends of one pair. (b) Optimized readout assignment error ε_{RO} for each transmon, with $\tau_{RO} = 400$ ns for all and τ_p is optimized for each. (c) Corresponding cumulative distribution function. The mean is 1.92% when including all transmons (dashed line), and 1.45% when excluding X_2 and X_4 (dotted line), whose readout is affected by known extraneous factors (see main text).

shoelacing with transmon frequency trimming by laser annealing reliably achieves fast, high-fidelity readout in multi-transmon processors. Due to the high yield of shoelace plucking, the time required to trim a full device is roughly linear in the number of resonators within. In future work, the process could be fully automated, for example, using the same automatic probe station used for laser annealing. We believe that the simplicity and reliability of shoelacing may find uses in microwave-engineering applications beyond circuit QED, including narrow-band matched filters, cameras based on kinetic-inductance detector arrays, and parametric amplifiers, to name a few examples.

See the supplementary material for fabrication details, the derivation of Eq. (3), the impact of the shoelacing on the resonator intrinsic quality factor, the laser annealing process used for transmon frequency trimming, the readout optimization and characterization procedures, and information on the devices used.

AUTHOR DECLARATIONS
Conflict of Interest

The authors have no conflicts to disclose.

Author Contributions

S.V.S. and S.L.M.M. contributed equally to this work.

S.V.S. and S.L.M.M. performed the experiment and data analysis. S.V.S, M.B. and L.D.C. conceptualized the experiment. M.B., N.H., S.V.S., and L.D.C. designed the devices. M.F., C.Z. and H.M.V. fabricated the devices with support from T.S.. S.L.M.M. and N.M. built the laser annealing setup. J.F.M. and H.A. acquired the data in Fig. 3. S.V.S. and L.D.C. wrote the manuscript with contributions from S.L.M.M. and M.F., with feedback from all coauthors. L.D.C. supervised the project.

Santiago Vallés-Sanclemente: Conceptualization (supporting); Data curation (equal); Formal analysis (equal); Investigation (equal); Methodology (equal); Visualization (equal); Writing – original draft (equal); Writing – review & editing (equal). **Thijs Stavenga:** Resources (supporting). **Nadia Haider:** Supervision (equal). **Leonardo DiCarlo:** Conceptualization (equal); Supervision (lead); Writing – original draft (equal); Writing – review & editing (equal). **Sean Louis Marien van der Meer:** Conceptualization (supporting); Data curation (equal); Formal analysis (equal); Investigation (equal); Methodology (equal); Software (equal); Visualization (equal); Writing – original draft (supporting). **Matvey Finkel:** Investigation (equal); Resources (equal); Writing – original draft (supporting). **Nandini Muthusubramanian:** Conceptualization (supporting); Resources (supporting). **Marc Beekman:** Conceptualization (equal); Resources (supporting). **Hany Ali:** Investigation (supporting); Methodology (supporting); Validation (supporting). **Jorge Miguel Ferreira Marques:** Investigation (supporting); Methodology (supporting); Validation (supporting). **Christos Zachariadis:** Resources (equal). **Hendrik Martijn Veen:** Resources (equal).

DATA AVAILABILITY

The data that support the findings of this study are openly available in the public repository DiCarloLab-Delft/Post_Fabrication_

Trimming_Data at http://github.com/DiCarloLab-Delft/Post_Fabrication_Trimming_Data, Ref. 26.

REFERENCES

[1] J. Hertzberg, E. Zhang, S. Rosenblatt, E. Magesan, J. Smolin, J. Yau, V. Adiga, M. Sandberg, B. M, J. M. Chow, and J. S. Orcutt, npj Quantum Inf. 7(1), 129 (2021).

[2] S. Krinner, N. Lacroix, A. Remm, A. Di Paolo, E. Genois, C. Leroux, C. Hellings, S. Lazar, F. Swiadek, J. Herrmann, G. J. Norris, C. K. Andersen, M. Müller, A. Blais, C. Eichler, and A. Wallraff, Nature 605, 669 (2022).

[3] E. Magesan and J. M. Gambetta, Phys. Rev. A 101, 052308 (2020).

[4] M. Ware, B. R. Johnson, J. M. Gambetta, T. A. Ohki, J. M. Chow, and B. Plourde, arXiv:1905.11480 (2019).

[5] V. Tripathi, M. Khezri, and A. N. Korotkov, Phys. Rev. A 100, 012301 (2019).

[6] J. F. Marques, B. M. Varbanov, M. S. Moreira, H. Ali, N. Muthusubramanian, C. Zachariadis, F. Battistel, M. Beekman, N. Haider, W. Vlothuizen, A. Bruno, B. M. Terhal, and L. DiCarlo, Nat. Phys. 18, 80 (2022).

[7] E. H. Chen, T. J. Yoder, Y. Kim, N. Sundaresan, S. Srinivasan, M. Li, A. D. Córcoles, A. W. Cross, and M. Takita, Phys. Rev. Lett. 128, 110504 (2022).

[8] S. Krinner, S. Lazar, A. Remm, C. Andersen, N. Lacroix, G. Norris, C. Hellings, M. Gabureac, C. Eichler, and A. Wallraff, Phys. Rev. Appl. 14, 024042 (2020).

[9] N. Muthusubramanian, A. Bruno, B. Tarasinski, A. Fognini, R. Hagen, and L. DiCarlo, American Physical Society March Meeting B29.015 (2019; available at https://meetings.aps.org/Meeting/MAR19/Session/B29.15

[10] E. J. Zhang, S. Srinivasan, N. Sundaresan, D. F. Bogorin, Y. Martin, J. B. Hertzberg, J. Timmerwilke, E. J. Pritchett, J.-B. Yau, C. Wang, W. Landers, E. P. Lewandowski, A. Narasgond, S. Rosenblatt, G. A. Keefe, I. Lauer, M. B. Rothwell, D. T. McClure, O. E. Dial, J. S. Orcutt, M. Brink, and J. M. Chow, Sci. Adv. 8, eabi6690 (2022).

[11] H. Kim, C. Jünger, A. Morvan, E. S. Barnard, W. P. Livingston, M. V. P. Altoé, Y. Kim, C. Song, L. Chen, J. M. Kreikebaum, D. F. Ogletree, D. I. Santiago, and I. Siddiqi, Appl. Phys. Lett. 121, 142601 (2022).

[12] D. M. Pozar, Microwave Engineering, 3rd ed. (John Wiley & Sons, Hoboken, 2005).

[13] M. Göppl, A. Fragner, M. Baur, R. Bianchetti, S. Filipp, J. M. Fink, P. J. Leek, G. Puebla, L. Steffen, and A. Wallraff, J. Appl. Phys. 104, 113904 (2008).

[14] M. Jerger, S. Poletto, P. Macha, U. Hübner, E. Il'ichev, and A. V. Ustinov, Appl. Phys. Lett. 101, 042604 (2012).

[15] J. Heinsoo, C. K. Andersen, A. Remm, S. Krinner, T. Walter, Y. Salathé, S. Gasparinetti, J.-C. Besse, A. Potočnik, A. Wallraff, and C. Eichler, Phys. Rev. Appl. 10, 034040 (2018).

[16] A. A. Houck, J. A. Schreier, B. R. Johnson, J. M. Chow, J. Koch, J. M. Gambetta, D. I. Schuster, L. Frunzio, M. H. Devoret, S. M. Girvin, and R. J. Schoelkopf, Phys. Rev. Lett. 101, 080502 (2008).

[17] M. Sandberg, F. Persson, I. C. Hoi, C. M. Wilson, and P. Delsing, Phys. Scr. 2009, 014018.

[18] R. Versluis, S. Poletto, N. Khammassi, B. Tarasinski, N. Haider, D. J. Michalak, A. Bruno, K. Bertels, and L. DiCarlo, Phys. Rev. Appl. 8, 034021 (2017).

[19] D. J. Thoen, B. G. C. Bos, E. A. F. Haalebos, T. M. Klapwijk, J. J. A. Baselmans, and A. Endo, IEEE Trans. Appl. Supercond. 27, 1500505 (2017).

[20] C. Macklin, K. O'brien, D. Hover, M. Schwartz, V. Bolkhovsky, X. Zhang, W. Oliver, and I. Siddiqi, Science 350, 307 (2015).

[21] J. Koch, T. M. Yu, J. Gambetta, A. A. Houck, D. I. Schuster, J. Majer, A. Blais, M. H. Devoret, S. M. Girvin, and R. J. Schoelkopf, Phys. Rev. A 76, 042319 (2007).

[22] P. Krantz, M. Kjaergaard, F. Yan, T. P. Orlando, S. Gustavsson, and W. D. Oliver, Appl. Phys. Rev. 6, 021318 (2019).

[23] J. Gambetta, A. Blais, M. Boissonneault, A. A. Houck, D. I. Schuster, and S. M. Girvin, Phys. Rev. A 77, 012112 (2008).

[24] T. Walter, P. Kurpiers, S. Gasparinetti, P. Magnard, A. Potočnik, Y. Salathé, M. Pechal, M. Mondal, M. Oppliger, C. Eichler, and A. Wallraff, Phys. Rev. Appl. 7, 054020 (2017).

[25] C. C. Bultink, M. A. Rol, T. E. O'Brien, X. Fu, B. C. S. Dikken, C. Dickel, R. F. L. Vermeulen, J. C. de Sterke, A. Bruno, R. N. Schouten, and L. DiCarlo, Phys. Rev. Appl. 6, 034008 (2016).

[26] See http://github.com/DiCarloLab-Delft/Post_Fabrication_Trimming_Data for the public repository with the data supporting the findings of this study.

08 August 2023 08:25:50